

GALEX UV COLOR-MAGNITUDE RELATIONS AND EVIDENCE FOR RECENT STAR FORMATION IN EARLY-TYPE GALAXIES

S. K. YI,^{1,2,3} S.-J. YOON,^{2,3} S. KAVIRAJ,³ J.-M. DEHARVENG,⁴ R. M. RICH,⁵ S. SALIM,⁵ A. BOSELLI,⁴ Y.-W. LEE,² C. H. REE,² Y.-J. SOHN,² S.-C. REY,^{2,6} J.-W. LEE,¹¹ J. RHEE,^{2,6} L. BIANCHI,⁷ Y.-I. BYUN,² J. DONAS,⁴ P. G. FRIEDMAN,⁶ T. M. HECKMAN,⁷ P. JELINSKY,¹² B. F. MADORE,^{8,9} R. MALINA,⁴ D. C. MARTIN,⁶ B. MILLIARD,⁴ P. MORRISSEY,⁶ S. NEFF,¹³ D. SCHIMINOVICH,¹⁰ O. SIEGMUND,¹² T. SMALL,⁶ A. S. SZALAY,⁷ M. J. JEE,⁷ S.-W. KIM,² T. BARLOW,⁶ K. FORSTER,⁶ B. WELSH,¹² & T. K. WYDER⁶

Accepted May 26 2004

ABSTRACT

We have used the GALEX UV photometric data to construct a first near-ultraviolet (NUV) color-magnitude relation (CMR) for the galaxies pre-classified as early-type by SDSS studies. The NUV CMR is a powerful tool for tracking the recent star formation history in early-type galaxies, owing to its high sensitivity to the presence of young stellar populations. Our NUV CMR for UV-weak galaxies shows a well-defined slope and thus will be useful for interpreting the restframe NUV data of distant galaxies and studying their star formation history. Compared to optical CMRs, the NUV CMR shows a substantially larger scatter, which we interpret as evidence of recent star formation activities. Roughly 15% of the recent epoch ($z < 0.13$) bright ($M[r] < -22$) early-type galaxies show a sign of recent ($\lesssim 1$ Gyr) star formation at the 1–2% level (lower limit) in mass compared to the total stellar mass. This implies that low level residual star formation was common during the last few billion years even in bright early-type galaxies.

Subject headings: galaxies: evolution — galaxies: star formation — ultraviolet: galaxies

1. INTRODUCTION

Color-magnitude relations (CMRs) have been widely-applied tools for studying the star formation history (SFH) in early-type galaxies and, in turn, for placing constraints on galaxy formation scenarios (monolithic vs. hierarchical). In optical colors, they show that brighter early-type galaxies are generally redder (Baum 1959; Sandage & Visvanathan 1977). It is often attributed to a metallicity sequence in the sense that brighter early-types are more metal-rich (Larson 1974; Bressan et al. 1994; Kodama & Arimoto 1997); but different scenarios, where age plays an important role, have also been proposed (Kauffmann & Charlot 1998; Kaviraj et al. 2004).

The UV light of an integrated population is a good tracer of recent star formation (RSF). Thus, find-

ing the local CMR is important: we can derive the SFH in early-types by comparing it to the galaxies at various redshifts (Bower et al. 1992; Stanford et al. 1998; van Dokkum et al. 1999; Ferreras & Silk 2000; Menanteau et al. 2002). The scatter in the CMR is also important. It is found to be small in optical CMRs (Bower et al. 1992). Because U -band light is relatively sensitive to the presence of young stars, Bower et al. (1992) interpreted the small scatter as an evidence of absence of recent major star formation activities in early-types. This result seemed a solid supporting evidence for the monolithic scenario.

The near-UV (NUV) light is far more sensitive to the presence of younger stars than the U band and thus traces RSF history better. The first internal-release data (IR0.2) from the GALEX project (Martin et al. 2004) contain the NUV data of nearby galaxies that are large enough for statistically significant investigations. It is our goal to derive a first NUV vs optical CMR for the present and recent epoch early-type galaxies based on this data and investigate their RSF history.

2. SAMPLE

GALEX is undertaking two wide-area surveys of different depth (Morrissey et al. 2004). The All-sky Imaging Survey (AIS) reaches limiting magnitudes 19.9AB in the far-UV (FUV, 1344–1786Å) and 20.8AB in the NUV (1771–2831Å), while the Medium Imaging Survey (MIS) reaches 22.6AB and 22.7AB in the FUV and NUV, respectively. For nearby galaxies, GALEX operates in the Nearby Galaxy Survey (NGS) mode applying the MIS exposure time. As an illustration, the colors of objects detected in one MIS field are displayed in Fig.1. Stars (dots mainly in the vertical sequence in the lower right) are separated from galaxies (crosses) clearly. The big galaxy clump in the upper middle of the plot shows

¹ Email: yi@astro.ox.ac.uk

² Center for Space Astrophysics, Yonsei University, Seoul 120-749, Korea

³ Department of Physics, University of Oxford, Oxford OX1 3RH, UK

⁴ Laboratoire d'Astrophysique de Marseille, 13376 Marseille Cedex 12, France

⁵ Department of Physics and Astronomy, UCLA, LA, CA 90095

⁶ California Institute of Technology, MC 405-47, Pasadena, CA 91125

⁷ Department of Physics and Astronomy, The Johns Hopkins University, Baltimore, MD 21218

⁸ Observatories of the Carnegie Institution of Washington, 813 Santa Barbara St., Pasadena, CA 91101

⁹ NASA/IPAC Extragalactic Database, California Institute of Technology, Mail Code 100-22, 770 S. Wilson Ave., Pasadena, CA 91125

¹⁰ Department of Astronomy, Columbia University, MC 5246, New York, NY 10027

¹¹ Department of Astronomy and Space Sciences, Sejong University, Seoul 143-747, Korea

¹² Experimental Astrophysics Group, Space Sciences Laboratory, UC Berkeley, Berkeley, CA 94720

¹³ Laboratory for Astronomy and Solar Physics, NASA Goddard Space Flight Center, Greenbelt, MD 20771

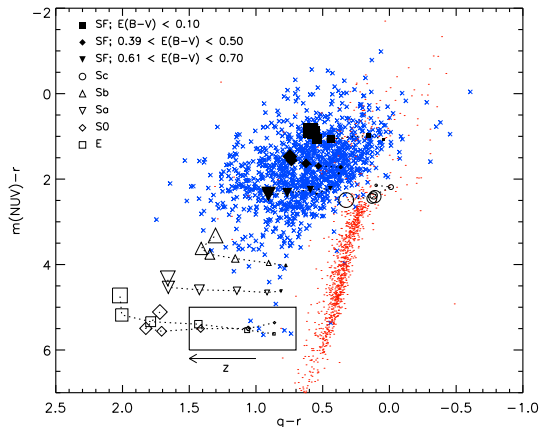


FIG. 1.— One GALEX MIS field data show a clear distinction between stars (*dots*) and galaxies (*crosses*). The expected positions for typical galaxies from star-forming galaxies (filled symbols) to quiescent early-type galaxies (open squares) are also depicted for $z = 0 - 0.5$ (from right to left). Low-redshift quiescent early-types are supposed to be faint in the UV and expected to be found in the square box. Optical data are from the SDSS database.

various galaxies currently star-forming, while quiescent early-type galaxies would be located in the lower part of the figure in and around the square box. The various symbols show the expected colors from the Kinney-Calzetti Spectral Atlas of Galaxies (Calzetti & Kinney 1994) for redshift 0–0.5 from right to left (arrow). If early-types are quiescent as often assumed, it would be an easy task to find them in this two-color diagram.

In order to construct a sample unbiased by any specific search criterion, we search for GALEX detections of galaxies already classified as being early-type by one of the major SDSS studies (Bernardi et al. 2003a). The Bernardi et al. classification is mainly based on concentration index, luminosity profile, and spectra with PCA classification. We use SExtractor’s MAG_AUTO (total) magnitudes from the GALEX catalog and Bernardi et al.’s *model* (total) magnitudes for optical bands. Our initial cross-identification of sources between the Bernardi et al. sample and the GALEX catalog results in 207 matches. We have removed 8 and 37 matches for having a close neighbor within 6 arcsec in GALEX and SDSS images, respectively. As a result, we have a total of 162 matches (133 from MIS, 18 from AIS, 11 from NGS). Of these, 62 have both FUV and NUV detections. Typical errors are 0.1 mag in NUV and 0.2 mag in FUV. These galaxies are at $z = 0 - 0.25$. It is from this final sample that we construct our NUV CMR.

3. UV CMR

We use the SDSS r (Fukugita et al. 1996) and GALEX NUV photometry to construct our CMRs (Fig.2). The top panel shows the whole sample, while the others show galaxies in different redshift bins. The absolute magnitudes are computed based on the distance derived from redshift, assuming $(\Omega, \Lambda, H_0) = (0.3, 0.7, 70)$. The uncertainty in the redshift is 0.001–0.002, and thus the uncertainty in the derived distance is negligible (Bernardi et al. 2003a). Extinction is from the Galactic correction of Schlegel et al. (1998); we make no correction for internal extinction. Because we do not assume to

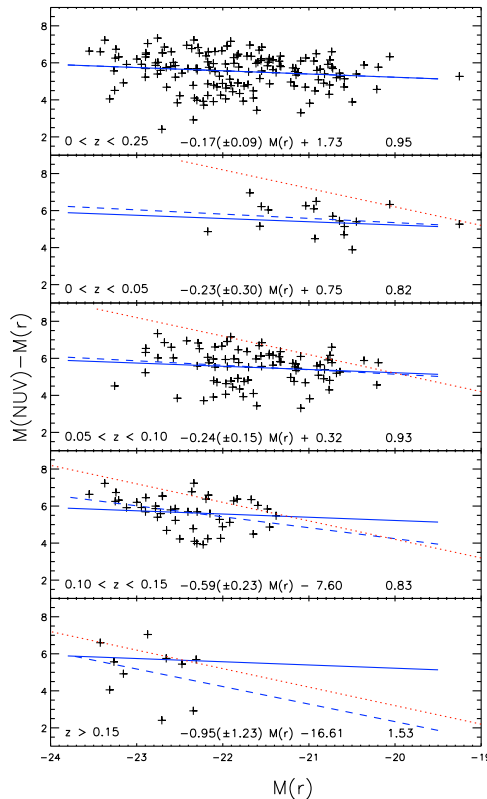


FIG. 2.— The UV CMR for all (top) and various redshift bins. The slope, intercept, and scatter of the data in each panel are written at the bottom. The fit to the whole data is shown in all panels as a solid line; the fit in each redshift bin is shown as a dashed line; and the detection limit as a dotted line.

know the spectral shapes of these galaxies a priori, we apply k -corrections based on the luminosity distance only. The k -corrections on the colors would be 0.1–0.2 mag. The fitting function to the whole and binned samples and the scatter (the standard error between the fit and the data), based on the first-order polynomial fitting, are shown at the bottom of each panel. At first sight, it appears that the slope (dashed line) gets monotonically steeper with redshift. But, this is an artifact due to the limiting magnitude affecting the completeness of the data. The data are roughly consistent with the global slope in all bins. The change of the slope is an important issue for studying the SFH of galaxies, but the sample needs to reach deeper to assert it.

The most notable feature in the UV CMR is its large scatter. The scatter in the NUV CMR (≈ 1 mag) is far greater than that found in any previous optical CMRs; e.g., the Bernardi et al. sample shows a $g - r$ scatter $\sigma_{RMS} = 0.05$ mag (Bernardi et al. 2003b). Only part of this scatter can be attributed to the photometric uncertainty (0.1 mag in NUV) and the k -correction on the colors (0.15 mag at $z = 0.2$). In order to understand the cause of the scatter, we divide the whole sample into three groups based on the NUV and FUV fluxes compared to the optical flux. Fig.3 summarizes our spectral classification scheme. The horizontal lines in the UV for the continuum fitting (right panels) show the criteria.

The first group, the “UV-weak” galaxies, show a

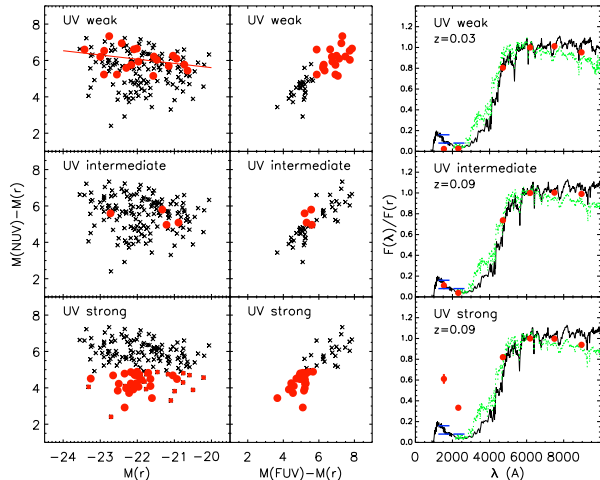


FIG. 3.— Three groups of early-type galaxies based on the UV spectral shape: “UV-weak” (top row), “UV-intermediate” (middle), and “UV-strong” (bottom). A linear fit to the UV-weak galaxies is shown in the top left panel and described in Eqn.1. In each panel, *crosses* are the whole sample, and *circles* are the galaxies in each group, and large *circles* are those with both FUV and NUV detections. In the right panels (shown in λ vs F_λ format), a typical example galaxy data (GALEX UV and SDSS optical photometry) for each group are shown. The reference SEDs are those of M32 (dotted) and of NGC 4552 (solid).

low UV flux: that is, $F(NUV)/F(r) < 0.08$ and $F(FUV)/F(r) < 0.08$. This originates from the upper bound in the NUV flux measured from Burstein et al. (1988)’s nearby quiescent elliptical sample and to a flat UV spectrum. Twenty out of 62 galaxies with both FUV and NUV data are classified in this group. They form the “red envelope” in the UV CMR in Fig.3 top left panel). The first order polynomial fit to the UV-weak galaxies is also shown and can be described as

$$M(NUV) - M(r) = -0.23(\pm 0.16) M(r) + 0.95, \quad (1)$$

which is consistent with the expected position of the quiescent ellipticals shown as a box in Fig.1. The standard error between the fit and the data is 0.58 mag. One can compare this quiescent early-type galaxy UV CMR to the observed optical CMR of high redshifts and derive the star formation history. The SED of an example galaxy is shown in the top right panel, in comparison to two reference SEDs of NGC4552 (a nearby UV-upturn galaxy) and of M32. The UV-weak galaxies are commonly suspected to be composed mainly of old stars.

We classify 4 out of 62 in the sample with both FUV and NUV detections as the “UV-intermediate group”. Their NUV flux is low, that is, $F(NUV)/F(r) < 0.08$; but their FUV flux is stronger than NUV, i.e., $0.08 < F(FUV)/F(r) < 0.16$, which is typical for nearby elliptical galaxies that show a UV-upturn (Burstein et al. 1988). Extremely old populations may be capable of developing such a moderate FUV flux (Yi et al. 1999; O’Connell 2000); but, it is difficult to determine whether their UV flux is indeed caused by young stars or old ones. Compared to the FUV light, the NUV light is less affected by the presence of old UV-bright stars and makes a safer tracer for RSF. We simply put these galaxies into

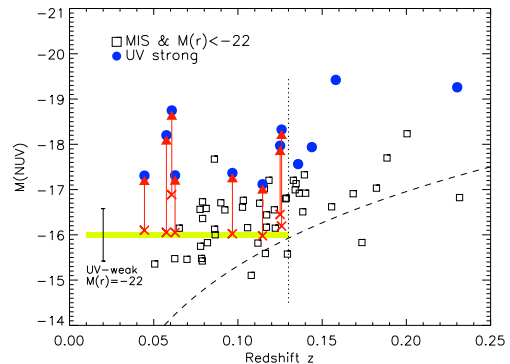


FIG. 4.— Bright ($M(r) < -22$) early-types in GALEX MIS fields. Filled circles denote the UV-strong galaxies. The dashed curve marks the detection limit of 23mag. The shaded thick horizontal line at $M(NUV) = -16$ with error bar ($\sigma=0.58$) shows the $M(NUV)$ for quiescent galaxies of $M(r)=-22$ expected from the UV-weak fitting function in Eqn.1. Seven UV-strong early-types are brighter in the UV than expected by the quiescent models (*crosses*) for their optical brightness ($M(r)$). Their departure (shown by vertical arrows) is probably due to a low level residual star formation in the recent past.

this category based on the UV spectral criteria without discussing their origin in this paper. They occupy the middle part of the data below the UV red envelope sequence (middle panels of Fig.3), contributing to the scatter of the CMR.

The last “UV-strong group” show strong UV flux (bottom right panel) either in the NUV *or* in the FUV in a manner that is unlikely to have come from old stars: that is, $F(NUV)/F(r) > 0.08$ *or* $F(FUV)/F(r) > 0.16$. Forty four galaxies are classified to be in this group, while 4 of them had no FUV detection. A sub-group of galaxies show a UV-upturn-type spectral slope, i.e., strong in the FUV and weak in the NUV, but a far stronger UV flux than any present epoch elliptical galaxy exhibits. An example is shown in Fig.3 bottom right panel. Note that the optical photometric data of this galaxy are close to those of typical elliptical galaxies, but its UV flux is significantly brighter. Such galaxies would not appear abnormal in optical CMRs but make themselves conspicuous in the UV CMR. A 2-component (old and young) χ^2 test on the GALEX and SDSS data indicates a recent starburst age of 0.2 Gyr having 1.2% of the total mass. For this test, we assumed that the dominant underlying population formed at $z = 5$ and of solar metallicity. Their high UV flux seems to be hinting at the presence of young (order of 100 Myr) stars. A larger fraction of galaxies in fact show a strong NUV flux, indicating the presence of 0.3 to 1 Gyr-old populations. The UV spectral slope (FUV–NUV) tells us the age of the RSF; and it is clear that the UV-strong galaxies are the prime culprit of the scatter in the UV CMR. Such a star-formation signature in early-type galaxies has been suggested by Deharveng et al. (2002) who used the FOCA data.

Then, we wonder what fraction of our galaxies are showing RSF signature. In order to answer this question, *we need to define a subsample whose red-envelope has*

been detected. Fig.4 shows only the bright ($M[r] < -22$) galaxies from GALEX MIS fields. For $z < 0.13$, GALEX reached their red envelope; that is, their predicted NUV magnitudes assuming they are UV-weak. Out of 41 such close bright galaxies, 8 (20%) are classified as UV-strong. The *crosses* denote their quiescent positions corresponding to their r -magnitudes adopting the UV-weak galaxy CMR in Fig.3. Their departure from the quiescent models (vertical arrows) can be explained by a low level RSF. As a supporting evidence, 6 of these 8 galaxies show a weak H_α emission line (see also Salim et al. 2004).

Since galaxy catalogs are in general subject to contamination of misclassified objects (Gavazzi et al. 2000; Shimasaku et al. 2001), we visually inspected the SDSS r -band images of all our galaxies. We find most of our UV-weak and UV-intermediate galaxies have early-type morphology but roughly 30% of UV-strong galaxies show ambiguous morphology, while still fitting the de Vaucouleurs profile. More distant galaxies are obviously more difficult to classify. For example, two of the 8 UV-strong galaxies in Fig.4 appear to be spiral. Some galaxies, which clearly appear to be early-type, show minor non-smooth features. Such features warn us about galaxy misclassification but might also be expected if the early-type galaxies experienced a merger event which caused RSF. Further investigation on their morphology, especially using multiband data, seems essential. When the two spiral-looking galaxies are removed from the UV-strong sample, our UV-strong fraction becomes 15% (6/39).

The NUV spectral signature as a sign of RSF remains apparent only for 1.5 Gyr or so. In other words, our NUV flux analysis detects only roughly a 1.5 Gyr or younger starburst. The typical mass fraction of the young populations in these RSF galaxies is 1–2%, based on our simple 2-starburst analysis. If the recent burst was not instant but extended, the 1–2% estimate should increase. In this regard, this value is a lower limit.

4. DISCUSSION

We have constructed a first UV CMR at present and recent epochs at $z = 0 - 0.25$. One can now compare this empirical UV CMR to higher redshift early-type galaxy data and derive their star formation history. Based on our sample, roughly 15% of bright ($M[r] < -22$) early-type galaxies show a RSF signature in the UV contin-

uum. This effectively rules out extreme versions of monolithic galaxy formation models where *all* stars form at high redshifts. The 15% estimate is a lower limit in the sense that our sample relies on Bernardi et al's classification, which excluded galaxies showing strong emission-lines (Fukugita et al. 2004). In addition, the internal extinction, which we ignored in this study, must have reduced the UV flux in some galaxies.

Recent semi-analytic models based on Λ CMD dynamics appear to be compatible with our discovery. For instance, Kaviraj et al. (2004) suggested that roughly 5–10% — depending strongly on the galaxy mass and environment — of the entire star formation in all (bright and faint) early-types happened at $z < 1$. The merger rate and the amount of residual star formation are predicted to be a sharply-increasing function of redshift (Khochfar & Burkert 2001), which is supported by observational studies (Menanteau et al. 2002; Bell et al. 2003). A detailed test against galaxy evolution models using GALEX data will be presented shortly.

An obvious next question is what triggers residual star formation. If it is a merger event, some UV-strong galaxies with a very young RSF might show morphologically disturbed features, as shown in HI gas map of the nearby elliptical galaxy, Cen A (Schiminovich et al. 1994). A follow-up investigation would be called for.

The strength of the UV CMR study is that it can detect even sub-1% level RSF event very easily. During its 28-month mission, GALEX will collect an order of magnitude larger and deeper data than used here and provide critical information on the recent star formation history in early-type galaxies.

ACKNOWLEDGMENTS

GALEX (Galaxy Evolution Explorer) is a NASA Small Explorer, launched in April 2003. We gratefully acknowledge NASA's support for construction, operation, and science analysis for the GALEX mission, developed in cooperation with the Centre National d'Etudes Spatiales of France and the Korean Ministry of Science and Technology. We thank Mariangela Bernardi for useful information on her catalog and Sadegh Khochfar, Joseph Silk, Roger Davies, Ignacio Ferreras for valuable comments. We thank the referee for a number of constructive suggestions.

REFERENCES

- Baum, W. A., 1959, PASP, 71, 106
 Bell, E. F., Wolf, C., Meisenheimer, K., Rix, H.-W., Borch, A., Dye, S., Kleinheinrich, M., & McIntosh, D. H. 2003, ApJ, in press (astro-ph/0303394)
 Bernardi et al. 2003a, AJ, 125, 1817
 Bernardi et al. 2003b, AJ, 125, 1882
 Bower, R. G., Lucey, J. R., & Ellis, R. S. 1992, MN, 254, 601
 Bressan, A., Chiosi, C., & Fagotto, F. 1994, ApJS, 94, 63
 Burstein, D., Bertola, F., & Buson, L. M., Faber, S. M., & Lauer, T. R. 1988, ApJ, 328, 440
 Calzetti, D., Kinney, A.L., & Storchi-Bergmann, T. 1994, ApJ, 429, 582
 Deharveng, J.-M., Boselli, A., & Donas, J. 2002, A&A, 393, 843
 Ferreras, I. & Silk, J. 2000, ApJ, 541, L37
 Gavazzi, G., Franzetti, P., Scodreggio, M., Boselli, A., & Pierini, D. 2000, A&A, 361, 863
 Greggio, L., & Renzini, A. 1990, ApJ, 364, 35
 Fukugita, M., Ichikawa, T., Gunn, J. E., Doi, M., Shimasaku, K., & Schneider, D. P. 1996, AJ, 111, 1748
 Fukugita, M., Nakamura, O., Turner, E.L., Helmboldt, J., & Nichol, R. C. 2004, ApJ, 601, L127
 Kauffmann, G., & Charlot, S. 1998, MN, 294, 705
 Kaviraj, S., Devriendt, J., Ferreras, I., & Yi, S.K. 2004, MN, submitted; astro-ph/0401126
 Khochfar, S., & Burkert, A. 2001, 561, 517
 Kodama, T., & Arimoto, N. 1997, 320, 41
 Larson, R. B. 1974, MN, 169, 229
 Martin, D. C., et al., 2004, ApJ, present volume.
 Menanteau, F., Abraham, R.G., & Ellis, R.S. 2002, MN, 322, 1
 Morrissey, P., et al., 2004, ApJ, present volume.
 O'Connell, R. W. 2000, ARAA, 37, 603
 Salim, S. et al. 2004, ApJ, present volume.
 Sandage, A. & Vishvanathan, N., 1977, ApJ, 203, 707
 Schlegel, D. J., Finkbeiner, D. P., & Davis, M. 1998, ApJ, 500, 525
 Schiminovich, D., van Gorkom, J. H., van der Hulst, J. M., & Kasow, S. 1994, ApJ, 423, L101
 Shimasaku et al. 2001 AJ, 122, 1238
 Stanford, S., Eisenhardt, P., & Dickinson, M. 1998, ApJ, 492, 461

van Dokkum, P. G., Franx, M., Fabricant, D., Kelson, D. D., & Illingworth, G. D. 1999, ApJ, 520, L95
Yi, S., Lee, Y.-W., Woo, J.-H., Park, J.-H., Demarque, P., & Oemler, A. 1999, ApJ, 513, 128